Nuclear Physics B290 [FS20] (1987) 218–230
North-Holland, Amsterdam

CRITICAL EXPONENTS IN A MODEL OF DYNAMICALLY TRIANGULATED RANDOM SURFACES

F. DAVID[1], J. JURKIEWICZ[2], A. KRZYWICKI[3] and B. PETERSSON[4]

[1] *Service de Physique Théorique, CEN-Saclay, 91191 Gif sur Yvette, France*
[2] *Institute of Physics, Jagellonian University, 30059 Krakow, Poland*
[3] *Laboratoires de Physique Theorique*, Bât 211, Université Paris-Sud, 91405 Orsay, France*
[4] *Fakultät für Physik, Universität Bielefeld, 4800 Bielefeld, FR Germany*

Received 11 February 1987
(Revised 3 April 1987)

We calculate the mass gap and the susceptibility critical exponents, in a model of dynamically triangulated random surfaces, for various values of the model parameters. Strong coupling series as well as Monte Carlo simulation are used and we carefully compare results obtained with the two methods. The transitions between different phases of the model are examined.

1. Introduction

A model of dynamically triangulated random surfaces [1–3] received recently considerable attention. In particular, much effort has been made to determine numerically the critical exponents of the model [1, 3–9]. The main purpose of this somewhat technical paper is to check the reliability of the numerical methods employed. We get also some further insight into the dynamics of the model.

The model in question can be regarded as a discrete version of the Polyakov string model [10]. The integration over surfaces is replaced by the sum over gaussian embeddings in a d-dimensional space of all two-dimensional abstract simplicial lattices (triangulations) with a given topology. The basic idea is that integration over metrics can be described by summation over triangulations. Thus, the partition function is written

$$Z = \sum_{\mathrm{T}N} W(\mathrm{T}) z^N \int' \prod_j \left[(q_j/\pi)^\alpha \mathrm{d}^d x_j \right] \exp\left(- \sum_{\langle km \rangle} (x_k - x_m)^2 \right). \tag{1}$$

Here T stands for "triangulation" and $1/W(\mathrm{T})$ is the order of the symmetry group of T. The total number of vertices in the lattice is N. The position, in the embedding

* Laboratoire associé au CNRS.

0169-6823/87/$03.50 © Elsevier Science Publishers B.V.
(North-Holland Physics Publishing Division)

TABLE 1
Summary of strong coupling and Monte Carlo results for the critical fugacity z_c (the upper number) and for the susceptibility exponent γ (the lower number)

(d, α)	Strong coupling with $N_\Delta \leqslant 24$	Monte Carlo in (100, 500)	Monte Carlo in (30, 100)
(5, 0)	0.2465 to 0.2472	0.24700 ± 0.00005	0.24615 ± 0.00016
	> 0.10	0.13 ± 0.05 (0.17 ± 0.04)	-0.32 ± 0.05 (-0.26 ± 0.03)
(5, 25)	0.0662 to 0.0665	0.06649 ± 0.00003	0.06633 ± 0.00005
	0.10 to 0.30	0.27 ± 0.12 (0.25 ± 0.15)	0.03 ± 0.04
(5, 5)	0.0166 to 0.0167		
	0.15 to 0.30		
(10, 0)	0.540 to 0.544	0.5421 ± 0.0001	
	0.25 to 0.40	0.20 ± 0.06 (0.19 ± 0.07)	
(10, 5)	0.0400 to 0.0404	0.04017 ± 0.00002	
	0.45 to 0.55	0.49 ± 0.12 (0.52 ± 0.08)	
(10, 25)		$(9.21 \pm 0.02) \times 10^{-8}$	$(9.30 \pm 0.02) \times 10^{-8}$
		1.00 ± 0.05 (0.94 ± 0.1)	1.70 ± 0.13 (1.71 ± 0.07)

The figure in parentheses is the result obtained using the second method of estimating γ.

space, of the jth vertex is denoted x_j and its coordination number (number of nearest neighbours) is denoted q_j. The parameters α and z control the dynamics of the model. In this paper we consider surfaces with spherical topology only.

The above presentation of the model is reduced to the necessary minimum, since the model has been extensively discussed in refs. [1–9]. In particular it has been explained how to introduce Green functions and critical exponents. Furthermore, standard scaling arguments have been used [11] to show that all the exponents can be expressed in terms of the susceptibility exponent γ and the mass-gap exponent ν (or alternatively the fractal dimension $d_F = 1/\nu$).

In the next section we shall consider estimates of γ obtained from strong coupling series and from Monte Carlo simulations. The results appearing in the text are summarized in table 1. In sect. 3 we present new strong coupling results for ν and compare them with Monte Carlo data. We also comment on transitions between different phases of the model. Sect. 4 contains a summary and conclusions.

2. The susceptibility exponent

2.1. STRONG COUPLING SERIES

The discussion of this section follows ref. [1]. Let us briefly recall the technique which has been used there.

Putting a dot in the middle of each triangle and joining dots belonging to neighbour triangles one obtains the so-called dual lattice. The latter has the same

structure as a planar vacuum diagram of the $g\,\mathrm{tr}\,\phi^3$ theory with $g \sim \sqrt{z}$ [1,3]. All such diagrams of a given order and with the correct symmetry factor can be generated using the Schwinger-Dyson equations of the $g\,\mathrm{tr}\,\phi^3$ theory. Then, for each surface, one computes the determinant and the inverse of the laplacian operator. This enables one to calculate the series expansion of the partition function and consequently to get an estimate of the critical "fugacity" z_c and of γ for various (positive or negative) values of the dimensionality d and of the measure parameter α. A similar series expansion for the mean square extent (or gyration radius) of the surface will be used in the next section to obtain the mass-gap exponent ν.

We have extended the analysis of ref. [1] by constructing high temperature series up to 24 triangles, which corresponds to approximately 5×10^7 different surfaces (see also ref. [6]). As in ref. [1] the method of differential approximants and the ratio method have been used. It turns out that the results obtained from differential approximants are less stable for the exponent γ. Therefore we shall present here only the results produced by the ratio method, which are also more suitable for a comparison with those extracted from Monte Carlo simulations. Let us briefly recall the idea of the method. Let the nth term in the series for $Z = \sum_{n \geq 1} z^{n+3} Z_n$ behave as follows

$$Z_n \sim B z_c^{-n} n^{\gamma - 3} \left[1 + O(n^{-1})\right]. \tag{2}$$

Here $n = N - 3 = \frac{1}{2} N_\Delta - 1$, N_Δ denoting the number of triangles. We first take the ratio

$$C_n^{(1)} = Z_n / Z_{n-1} \sim z_c^{-1} \left[1 + (\gamma - 3)/n + O(n^{-2})\right]. \tag{3}$$

Next, we define

$$C_n^{(p+1)} = \left[n C_n^{(p)} - (n-p) C_{n-1}^{(p)}\right]/p \tag{4}$$

and use the fact that

$$C_n^{(p)} \sim z_c^{-1} \left[1 + O(n^{-p})\right], \tag{5}$$

to obtain better and better estimates of z_c, by extrapolating $C_n^{(p)}$ to $n = \infty$ for successive values of p.

Similarly, estimates for γ are obtained applying the same technique to

$$D_n^{(1)} = n \left[C_n^{(1)} - C_n^{(2)}\right]. \tag{6}$$

As an illustration let us consider the case $d = 10$ in some more detail. In figs. 1 and 2 we display the estimates $C_n^{(p)}$ for the position of the critical point, for $\alpha = 5$ (i.e. $= \frac{1}{2} d$) and $\alpha = 0$ respectively. Anticipating on the discussion of the next sub-section we also show the results of Monte Carlo simulations. For $\alpha = 5$ the convergence is quite good and the extrapolation to $n = \infty$ indicates the estimate $0.0400 < z_c < 0.0404$, to be compared with $z_c = 0.04017 \pm 0.00002$ obtained from

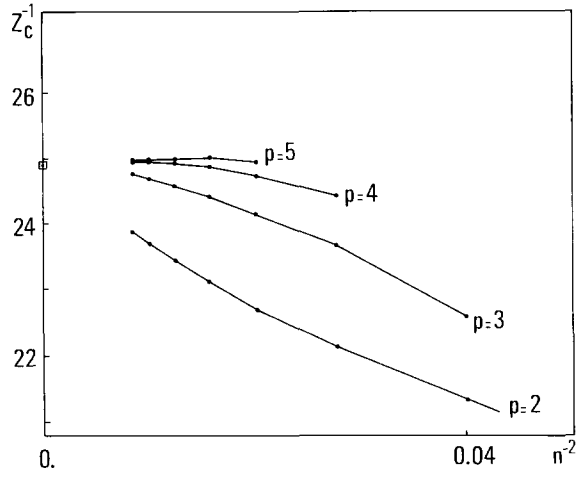

Fig. 1. Strong coupling estimates for the critical fugacity z_c at $d = 10$ and $\alpha = 5$. One should extrapolate to $n = \infty$. The Monte Carlo result is also shown (open square).

Monte Carlo. For $\alpha = 0$ the convergence is less good since one observes some drift with p. The estimate is $0.540 < z_c < 0.544$ to be compared with $z_c = 0.5421 \pm 0.0001$ from Monte Carlo.

In fig. 3 are plotted the estimates $D_n^{(p)}$ for γ, for $\alpha = 5$ and 0. For $\alpha = 5$ the convergence is again quite good, the estimates rather weakly depend on p, and one is led to conclude that $0.45 < \gamma < 0.55$ in agreement with $\gamma = 0.49 \pm 0.12$ obtained from Monte Carlo. The situation is less favourable for $\alpha = 0$: one observes a

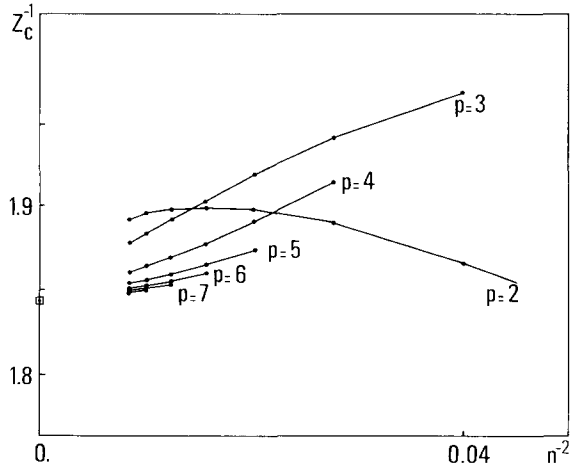

Fig. 2. The same as fig. 1 but for $\alpha = 0$.

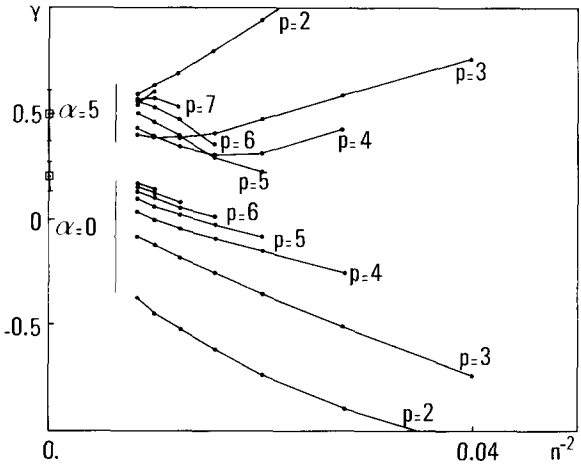

Fig. 3. Strong coupling estimates for the susceptibility critical exponent γ for $d = 10$ and $\alpha = 0$ and 5. Monte Carlo results are also shown (open squares).

systematic drift of estimates with p, towards larger and larger values, which makes the overall estimate of γ much less convincing. A naive extrapolation yields $0.25 < \gamma < 0.40$, a value significantly smaller than at $\alpha = 5$, but the upper bound is not very reliable and it is quite possible that γ is actually the same for $\alpha = 5$ and $\alpha = 0$. This estimate is again compatible with Monte Carlo result, $\gamma = 0.20 \pm 0.06$, especially that the error attached to the Monte Carlo point is in this case presumably underestimated, as will be discussed in the next subsection.

Notice that the systematic drift of estimates with the order p of the approximant is a typical phenomenon, occurring frequently when there is another singularity close to z_c, or a confluent singularity at z_c with an exponent $\gamma' < \gamma$. This can be shown explicitly in the solvable case $d = -2$, $\alpha = 0$, where a confluent singularity exists [12].

For values of α larger than 5, say near 10, the convergence of the ratio method is also less good. In this case the drift phenomenon leads to estimates of γ systematically above 0.5. For still higher values, say $\alpha = 25$, the estimates obtained from strong coupling series (of this length, of course) become completely unreliable.

We have performed a similar analysis at $d = 5$. As in the previous case the convergence is better for $\alpha = 5$ and 2.5 than for $\alpha = 0$. The estimates for z_c and γ are given in table 1. For $\alpha = 0$ we observe again the drift phenomenon and the estimate for γ is systematically lower, but less reliable, than for $\alpha = 2.5$ or 5. Again, the error in the Monte Carlo estimate of γ at $\alpha = 0$ is presumably too optimistic.

2.2. MONTE CARLO SIMULATIONS

2.2.1. General outlook. The code employed in this work has already been used in ref. [9], and is described in detail there. Here we shall discuss in more detail the

conditions, which in our opinion should be fulfilled to insure that an estimate of γ extracted from a simulation of the grand-canonical ensemble of random surfaces is reliable. Let us first briefly state how our computer simulations have been run:

The algorithm changes by ± 1 the number N of vertices. This biased random walk is constrained to a finite interval $N_{\min} < N < N_{\max}$ of length $\Delta N = N_{\max} - N_{\min}$. Denote by $Z_{\exp}(N)$ the frequency of occurrence of surfaces with N vertices in a simulation where one has attempted to update the surface t times. Since the algorithm obeys detailed balance, one has

$$Z_{\exp}(N) \sim z^N Z_N, \qquad N_{\min} \leqslant N \leqslant N_{\max} \tag{7a}$$

in the limit $t \to \infty$. In actual experiments, for convenience, the importance sampling method has been used to generate

$$Z_{\exp}(N) \sim N^3 z^N Z_N, \tag{7b}$$

which has the asymptotic behaviour

$$Z_{\exp}(N) \sim N^{\gamma} (z/z_c)^N \tag{8}$$

for $N \to \infty$ (cf. eq. (2), remembering that $N = n + 3$). In order to find γ, $\ln Z_{\exp}(N)$ has been fitted with $aN + b \ln N + c$; b is then an estimate of γ. Another estimate is given by the ratio of moments of $Z_{\exp}(N)$, with a correction for boundary effects (cf. eqs. (10)–(11) of ref. [9]). Each experiment has been repeated several times to allow an error estimate. The condition

$$(Et)^{1/2} \gg \Delta N, \tag{9}$$

(E is the acceptance rate of the algorithm) has been satisfied in each of these experiments, the left-hand side being larger than the right-hand side by at least a factor 20. The concordance, within errors, of the estimates obtained using the two methods mentioned above is among the conditions for these estimates to be considered reliable*.

It is obvious that for finite t there are quite strong correlations between values of $Z_{\exp}$ observed at two not too distant N's. If the system is at $N = N_0$ at a given moment, it has a finite probability to stay near N_0 for some time, producing a bump in $Z_{\exp}$. It takes a long time before such a bump disappears. We have observed pronounced bumps (or dips) extending over distances as large as 50, although the system had enough time to pass many times over the full interval.

* Following a suggestion by Koukiou and Petritis we have checked that the method proposed in ref. [13] yields estimates very close to those obtained with our techniques.

Now, assuming that (8) holds, one faces two related problems: one has to disentangle the power and the exponential factors and one has to distinguish physics from broad dips and bumps which can mock it.

We have been choosing z so as to produce an extremum in $Z_{\text{exp}}(N)$ within the interval $(N_{\text{min}}, N_{\text{max}})$. The extremum is produced by the competition between the linear and the logarithmic term in $\ln Z_{\text{exp}}(N)$ and its presence helps to disentangle these two terms. The extremum in question is usually very broad and can be clearly seen, superposed on the noise dips and bumps, when ΔN is large, say of the order of several hundreds. We have checked that one may obtain wrong results when such an extremum is absent, in spite of high statistics: In such cases because of fluctuations the best fit is achieved with a too small (large) z_c, compensated with the choice of a too small (large) γ.

Since z_c is a priori unknown, the value of z to work with is determined by trial and error, in a series of preliminary runs. Again, finding a suitable z is particularly easy when ΔN is large. Otherwise the fine tuning of z requires much computer time. One might think that by choosing a smaller ΔN one saves time, since the condition (9) is sooner satisfied. However, with too small a ΔN it is difficult to unravel the true trend of the data from noise. Consequently, one has to pass over the whole interval of N more times to smoothen the data and the would be gain of computer time is to large extent lost.

Following these general remarks, let us consider some specific cases of interest.

2.2.2. The variation of the effective γ with the size of surfaces. At $d = 5$ and $\alpha = 2.5$ (i.e. $= \frac{1}{2}d$) we first worked in the interval (100, 500) with $z = 0.0664$, obtaining $z_c = 0.06649 \pm 0.00003$, $\gamma = 0.27 \pm 0.12$ and $\gamma = 0.25 \pm 0.15$, from the two methods of estimating the susceptibility exponent. After $t = 4.8 \times 10^8$ ($E \approx 57\%$) steps we could observe a nice extremum of $Z_{\text{exp}}(N)$: first a rise by about 5% in (100, 200), then a broad maximum somewhere in (200, 300) followed by a steady decrease by about 15% in (300, 500). In order to check for finite size effects, we subsequently ran a simulation in the interval (30, 100). With no z could we obtain an extremum of $Z_{\text{exp}}(N)$. Setting $z = 0.0663$ and with $t = 2 \times 10^8$ we got a remarkably flat distribution (within $\pm 0.5\%$). In such a case the second method of estimating γ cannot be used: because of cancellations in the formula for γ (eq. (10) of ref. [9]) the estimate is too sensitive to the values taken by $Z_{\text{exp}}(N)$ at $N = N_{\text{min}}, N_{\text{max}}$. The best fit to the data yields $z_c = 0.06633 \pm 0.00005$ and $\gamma = 0.03 \pm 0.04$. The result for z_c is still in perfect agreement with the strong coupling estimate. However, γ compatible with zero is well outside the interval $0.10 < \gamma < 0.30$ quoted in the preceding subsection and is also significantly different from the Monte Carlo estimate extracted from the simulation in (100, 500).

We noticed a similar phenomenon at $\alpha = 0$. Working in the interval (100, 500) with $t = 7 \times 10^8$ ($E \approx 57\%$) we find $z_c = 0.24700 \pm 0.00005$ and the estimates for the susceptibility exponent $\gamma = 0.13 \pm 0.05$ and $\gamma = 0.17 \pm 0.04$, respectively. In the interval (30, 100) with $t = 2 \times 10^8$ we get $z_c = 0.24615 \pm 0.00016$, while the estimates

for γ are -0.32 ± 0.05 and -0.26 ± 0.03, again significantly lower than in (100, 500). We interpret these observations as an evidence for a finite size effect. The variation of the *effective* γ with the considered interval of N is not really surprising. For the solvable case $d = 0$ one finds that the sub-asymptotic terms are negligible for $N \gg 8$. For $d > 0$ the strong coupling series discussed in subsect. 2.1 already indicate that these sub-asymptotic terms are much more important than for $d = 0$. The pertinent question is whether these terms are negligible for $N > 100$ when $d = 5$ or 10. Unfortunately, we cannot offer a firm answer to this question. There exist arguments, based on Orstein-Zernicke equations, to the effect that $\gamma = \frac{1}{2}$ as soon as $\gamma > 0$ [2, 11, 14]. Our results do not exclude the possibility that the currently observed trend of the Monte Carlo data persists as N increases, until γ reaches this "mean field" value $\frac{1}{2}$. Let us mention, however, that in our microcanonical simulations [4–5], sizeable deviations from the simple scaling law $\langle r^2 \rangle \sim N^{2\nu}$ have also been observed for $N < 100$. Therefore, the rise of the effective γ reported above does not necessarily imply that the asymptotic regime has not been reached in the interval (100, 500).

2.2.3. The limit of large α. Another interesting finite size effect is encountered when one tries to explore the limit of large α for fixed d. Set $d = 5$ and let $\alpha = 25$. This value of α can be considered "large", since the typical change of $\alpha \Sigma_j \ln q_j$ under a "flip" of a link is of order unity. Thus, the price for curving the surface is high.

We first ran an exploratory simulation, working in the interval (30, 100). In spite of a modest statistic $t = 7.5 \times 10^7$ ($E \approx 27\%$) we got reliable estimates $z_c = (9.30 \pm 0.02) \times 10^{-8}$ and $\gamma = 1.7 \pm 0.1$, with both methods. Going over to the interval (100, 500) and with $t = 6 \times 10^8$ we find $z_c = (9.21 \pm 0.02) \times 10^{-8}$ and $\gamma = 1.00 \pm 0.05$ (the second method gives $\gamma = 0.94 \pm 0.1$). The difference with the preceding result is considerable. Furthermore, it is striking that γ overshoots $\frac{1}{2}$, the upper bound for generic surfaces [6, 15]. In order to get some insight into the structure of the relevant surfaces we extracted from our data the distribution of geodesic distances *within the lattice* between all pairs of surface points, for a sample of surfaces, using the method of ref. [7]. Notice that if r is such a distance, and as long as the finite size of the surface is not felt, then

$$\text{Prob}(r) \sim r^{\delta - 1}. \tag{10}$$

For a generic surface $\delta \geqslant 2$, while for a long tube $\delta = 1$. We display Prob(r) in fig. 4 for two typical surfaces with $N \approx 190$, one taken from a simulation at $\alpha = 0$ and the other from an experiment at $\alpha = 25$. At $\alpha = 0$ the distribution first rises fast with r, but on the whole is concentrated at small values of r. This is not a surprise, one is close to the phase of "crumpled" surfaces, where some points have large negative curvature and geodesic distances between points are small. This Prob(r) does not significantly broaden when N is increased to 400, or so. On the contrary, at $\alpha = 25$,

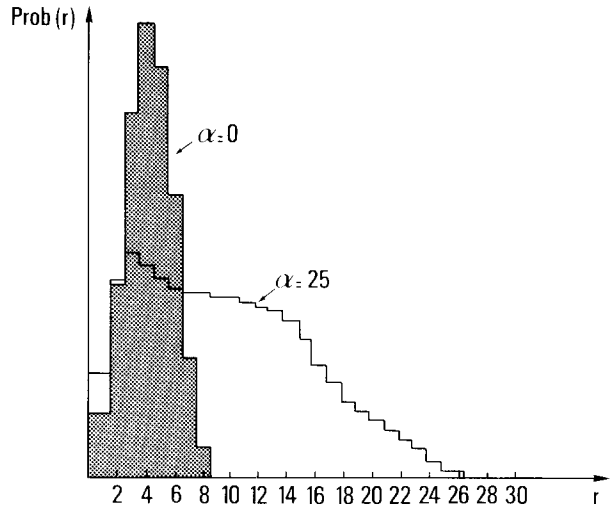

Fig. 4. The frequency of occurrence of different geodesic distances r between pairs of lattice points for typical sample lattices with $N \approx 190$ for $d = 5$, $\alpha = 0$ and 25.

Prob(r) has a noticeable (almost) flat part, indicating an elongated, cigar-like shape. The large r fall of the distribution reflects the finite size of the surface. The dip at small r shows that at small scales the overall cigar shape is not felt. The distribution broadens when N is increased.

Now, for a long tube, flat everywhere except at the end (see e.g. fig. 7 in ref. [8]), the partition function Z_N can be calculated analytically, for large N, and one finds $\gamma = 3$. It is easy to convince oneself that the argument leading to the bound $\gamma \leqslant \frac{1}{2}$ does not go through for such a surface. Our data at $\alpha = 25$ indicate that (roughly) cigar-shaped surfaces contribute significantly to the partition function. Notice, however, that the tubes would presumably branch if N were increased enough, so that the surface would take the shape of a branched polymer with $\gamma = \frac{1}{2}$. Letting α to be large, but finite, merely reduces the branching probability. The result of our simulation seems entirely controlled by a finite size effect: the branching had no opportunity to develop yet.

2.2.4. Slow convergence at $\alpha = 0$. While discussing the strong coupling results, we have pointed out the importance of the "drift" phenomenon for $\alpha = 0$. It appears that the dynamics responsible for this absence of manifest convergence of our strong-coupling estimates is also felt in the Monte Carlo simulations. Hence at $d = 10$ ($\alpha = 0$) our experiments yield results for γ roughly grouped near two values, viz. ≈ 0 and ≈ 0.4, with an indication for a correlation between successive experiments (thus the correlation extends over $\Delta t \sim 10^8$). With overall statistics of $t = 10^9$ ($E \approx 48\%$) we get the following results, which appear stable: $z_c = 0.5421 \pm 0.0001$ as well as $\gamma = 0.20 \pm 0.06$ and $\gamma = 0.19 \pm 0.07$ with the two methods, respectively. The

error estimates are obtained from 7 experiments with $t = 1.5 \times 10^8$ each. However, in view of the observed correlations the above error estimates are likely to be too optimistic. Grouping the results of measurements further in the standard fashion indicates that realistic errors might be twice larger. The results at $d = 5$ and $\alpha = 0$, mentioned earlier, also indicate rather slow convergence. We interpret this slow convergence observing that with these values of the model parameters one is entering the phase of "crumpled" surfaces. Apparently, when there appears a vertex with very large negative curvature it is difficult to get rid of it.

3. The mass-gap exponent

Although this paper does not present any new Monte Carlo estimate for the mass-gap exponent ν, we shall briefly discuss results of series analysis for ν. Indeed, in ref. [1] preliminary estimates for ν from strong coupling series have been presented, but these estimates were rather poor, since based on the assumption that ν is independent of the measure parameter α. Subsequent Monte Carlo simulations have shown that ν does in fact strongly depend on α [4–8]* and we believe it is interesting to present a more elaborate study of strong coupling results, to be compared with the data of refs. [4, 5].

For a given N, the average gyration radius can be written

$$\langle r^2 \rangle_N = \Omega^{-1} \sum_{\mathrm{T}} W(\mathrm{T}) \int' \prod_j \left[(q_j/\pi)^\alpha \, \mathrm{d}^d x_j \right] \exp\left\{ - \sum_{\langle l, m \rangle} (x_l - x_m)^2 \right\}$$

$$\times \sum_{k, m} q_k q_m (x_k - x_m)^2 . \tag{11}$$

The normalization factor Ω is

$$\Omega = 9 N_\Delta^2 Z_N , \tag{12}$$

where Z_N is the partition function for the fixed N.

We have analysed the strong coupling series for the gyration radius $\langle r^2 \rangle$ up to 24 triangles by the technique explained in subsect. 2.1. The estimates of ν are presented in fig. 5, for various values of α and for $d = 10$. The exponent ν depends indeed on α: it is fairly small for negative α (this corresponds to a very large fractal dimension since $\nu = 1/d_{\mathrm{F}}$, as already mentioned) and approaches the "mean field" value $\frac{1}{4}$ for not too small positive α (corresponding to fractal dimension 4 of branched polymers). In the same figure we have plotted the results of the Monte Carlo simulations of ref. [4] at $d = 10$ and of ref. [5] at $d = 12$ (the dependence of ν on d

* Actually, such a dependence was already suggested by the results of ref. [1], but has not been studied thoroughly there.

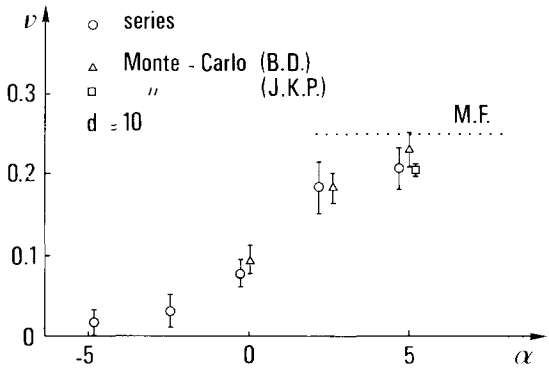

Fig. 5. The mass-gap exponent ν versus $\alpha(d=10)$: a comparison between strong coupling and Monte Carlo results.

is in fact weak near $d=10$). The agreement between Monte Carlo and series estimates is quite good and seems to favour a smooth dependence of ν on α. At this point one should remark that a similar strong coupling analysis for $d=-2$ and $\alpha=0$ yields ν larger than zero ($\nu=0.10\pm0.01$) while it has been recently proven by Kostov and Mehta [16] that for the surfaces considered here (no "tadpoles" and "self-energies" in the dual lattice) the exact value is $\nu=0$. Notice, however, that the ratio method is not really suitable for studying a logarithmic behaviour and that in a Monte Carlo simulation it is obviously difficult to distinguish $\log N$ from $N^{2\nu}$ when ν is very small, since one necessarily explores a finite interval of N. Thus, when a small value of ν is observed, say <0.1, it may mean that ν is actually zero.

In order to get further ideas about the dynamics of the crossover mentioned above, we have performed a microcanonical ensemble simulation at $d=10$, varying α by small steps, from $\alpha=-40$ to $\alpha=40$. The average scalar curvature squared $\langle R^2\rangle$ has been calculated for N_Δ ranging from 50 to 1000. This quantity depends weakly on α below $\alpha\approx-10$, where $\langle R^2\rangle\approx1.5$, and above $\alpha\approx20$, where $\langle R^2\rangle$ is very small. Between these two regimes $\langle R^2\rangle$ falls rapidly, but with no evidence for finite size effects. A similar analysis with analogous conclusions has been performed for $\langle\log q\rangle$.

For completeness we display in fig. 6 the variation of ν versus d (for $\alpha=\frac{1}{2}d$), which is also fairly smooth.

4. Discussion and summary

The sample results given in the preceding sections indicate a very satisfactory agreement between estimates obtained from strong coupling series and from Monte Carlo simulations, respectively. However, we have emphasised that the quality of these estimates is sensitive to the values taken by the parameters of the model. We

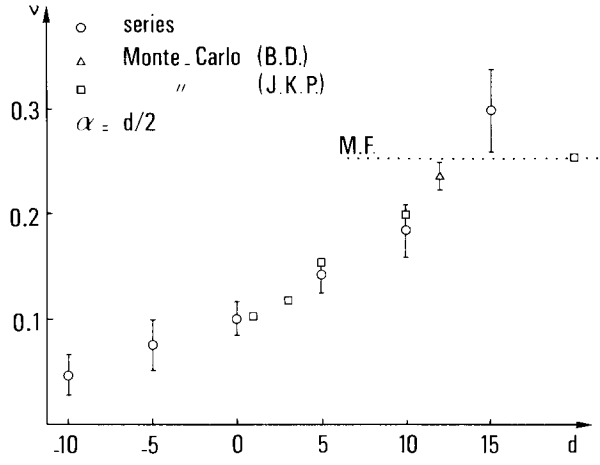

Fig. 6. The mass-gap exponent ν versus $d(\alpha = \frac{1}{2}d)$: a comparison between strong-coupling and Monte Carlo results.

have given on purpose many technical details concerning the methods used to get these estimates. Thus, the reader can judge by himself the significance of these (and other) results. Our data indicate that in order to get from Monte Carlo simulations serious estimates of critical exponents, hopefully insensitive to finite size effects, one should consider surfaces at least as large as these studied by us here (number of triangles $N_\Delta > 200$). This has already been noticed in refs. [4–5], in the context of microcanonical simulations designed to determine the mass-gap exponent, and is further confirmed by the results obtained here for the susceptibility exponent.

Concerning physics, we clearly see the transitions between different regimes, whose existence has been suggested in the literature, using analytic arguments [6, 8] holding for $|\alpha|, |d| \to \infty$ and also on the basis of numerical data. Thus, keeping d fixed (not too small) and varying α we observe the transition between "crumpled" surfaces (in the sense of ref. [8]) and branched polymers. On the other hand, changing d and α along the line $d = \frac{1}{2}\alpha$ the transition between Liouville surfaces and branched polymers is seen. When the variation of the mass-gap exponent is studied these transitions appear quite *smooth*. In spite of some effort in this direction, we have found no evidence that this observed smoothness is merely a finite size effect. The susceptibility exponent also varies smoothly in our data for $\alpha = 0$. However, as remarked in ref. [9], the transition from the regime with $\gamma < 0$ to the one where the "mean field" value $\gamma = \frac{1}{2}$ is reached, appears relatively rapid when $\alpha = \frac{1}{2}d$.

Only one class of models has been studied so far. However, the tools created for this purpose can easily be adapted to other models, possibly with more sophisticated actions. There is much work in perspective!

We wish to thank the Conseil Scientifique du Centre de Calcul Vectoriel pour la Recherche (CCVR) for granting us computing time on CRAY 1. We also acknowledge the support of the Bochum University Computing Center for using their CYBER 205. One of us (J.J.) acknowledges the support from the project CPBP 01.03.2.4.2.

References

[1] F. David, Nucl. Phys. B257 (1985) 543
[2] J. Ambjørn, B. Durhuus and J. Fröhlich, Nucl. Phys. B257 (1985) 433
[3] V.A. Kazakov, I.K. Kostov and A.A. Migdal, Phys. Lett. B157 (1985) 295
[4] J. Jurkiewicz, A. Krzywicki and B. Petersson, Phys. Lett. B168 (1986) 273
[5] A. Billoire and F. David, Phys. Lett. B168 (1986) 279
[6] J. Ambjørn, B. Durhuus and J. Fröhlich, Nucl. Phys. B275 (1986) 161
[7] A. Billoire and F. David, Nucl. Phys. B275 (1986) 617
[8] D.V. Boulatov, V.A. Kazakov, I.K. Kostov and A.A. Migdal, Phys. Lett. B174 (1986) 87; Nucl. Phys. B275 (1986) 641;
D.V. Boulatov and V.A. Kazakov, Moscow SRI preprint Pr-1122 (1986)
[9] J. Jurkiewicz, A. Krzywicki and B. Petersson, Phys. Lett. B177 (1986) 89
[10] A.M. Polyakov, Phys. Lett. B103 (1981) 207
[11] B. Durhuus, J. Fröhlich and T. Jonsson, Nucl. Phys. B240 (1984) 453
[12] F. David, unpublished
[13] A. Berretti and A.D. Sokal, J. Stat. Phys. 40 (1985) 483
[14] J. Fröhlich, *in* Recent developments in quantum field theory, eds. J. Ambjørn, B. Durhuus and J.L. Petersen (North-Holland, 1985)
[15] J. Ambjørn, B. Durhuus, J. Fröhlich and P. Orland, Nucl. Phys. B270 (1986) 457
[16] I.K. Kostov and M.L. Mehta, Saclay preprint SPhT/87-03 (1987)